Simulating the Effects of Serum Potassium on the ECG

Sanjay Kharche[1, 2], Giulia Callisesi[2], Tomas Stary[2], Andrea Bracci[2], Stefano Severi[2]

[1]University of Liverpool, Liverpool, UK, [2]University of Bologna, Cesena, Italy.

Abstract

The O'Hara et al. ventricular cell model was used to quantify cell and tissue electrical characteristics under altered extracellular serum potassium ($[K^+]_o$) levels. The cell model was incorporated into a heterogeneous 1D bi-domain virtual strand description where pseudo-ECG was computed. In multiple simulations, the effects of $[K^+]_o$ on CV and ECG T wave were quantified. Further, heterogeneous inter-cellular coupling was simulated to elicit the augmented action potential dispersion in human ventricles observed experimentally.

An increase of $[K^+]_o$ reduced APD_{90} and increased cellular alternans propensity. In 1D simulations, CV was reduced due to both increased and reduced $[K^+]_o$. ECG T wave amplitude and absolute value of repolarization slope reduced with increasing $[K^+]_o$.

There is a close correlation between ECG and $[K^+]_o$ which could be used in non-invasive diagnostic methods.

1. Introduction

Mortality in end stage chronic renal disease patients is largely due to the associated chronic cardiac disease. Cardiac arrythmogenesis is also a major side effect of renal therapy like hemodialysis. Indeed, clinical observations show an increased incidence of fatal arrhythmic paroxysms during hemodialysis, demonstrating the sub-optimal personalization of the therapy [1]. A non-invasive diagnostic procedure being preferred, clinical efforts continue to investigate the manifestation of dialysis in the ECG [2]. Complementary to clinical and experimental studies, the proarrhythmic effects of altered serum electrolyte levels are being studied using biophysically detailed models of human cardiac cells and tissue [3-5]. This computer modeling study extends the cellular modeling to tissue level to enable simulation of realistic ventricular component of the ECG. The unique feature of the model was a spatially dependent diffusion constant to simulate fiber orientation and the spatial dependence of gap junctional heterogeneity. A quantitative correlation between $[K^+]_o$ action potential (AP) characteristics, tissue conduction behaviour, and ECG features was computed by means of multiple simulations. Due to the computationally efficient methods used, the cell and tissue models allowed the necessary high throughput parameter sweep simulations.

2. Methods

The recently published O'Hara et al. (ORD) ventricle cell model [6] was used in this study. Electrical heterogeneity simulating endocardial (endo), M and epicardial (epi) action potentials (APs) was simulated according to the original publication. As the action potentials (APs) show rate dependent adaptation, the cell models were paced for 1000 beats when the AP was deemed to be stable. Using the cell models, the effects of altered $[K^+]_o$ on AP duration (APD_{90}) were simulated in a wide range of $[K^+]_o$ values. Dynamic APD_{90} restitution was computed by pacing the cell models at various pacing cycle lengths (PCL) and recording APD_{90} of the penultimate 10 excitations.

The cell models were incorporated into a 1D electrically and spatially heterogeneous bi-domain strand using the reaction-diffusion partial differential equation (PDE) [7]:

$$-C_m \frac{\partial V}{\partial t} = I_{ion}(x,t) + I_{app} + \frac{1}{\beta}\frac{\partial}{\partial x} D_e(x)\frac{\partial \phi}{\partial x} \quad \text{Eq. (1)}$$

$$\frac{\partial}{\partial x}\left((D_i(x) + D_e(x))\frac{\partial \phi}{\partial x}\right) = -\frac{\partial}{\partial x}\left(D_i(x)\frac{\partial V}{\partial x}\right)$$

where C_m is cell capacitance, V is cell membrane potential, I_{ion} is the reaction current, I_{app} is the applied current, β is the cell surface to volume ratio, D_e is the extracellular diffusion, D_i is the intracellular diffusion, and φ is the extracellular potential. In accordance with experimental data [8], the strand was taken to consist of 15 endocardial, 25 mid-myocardial, and 150 epicardial cells. The intercellular distance was assumed to be 0.1 mm. The value of C_m was taken to be 1 $\mu F/cm^2$ [6] and β to be 15 mm^{-1} [9-11] based on previous modelling studies. The values of D_e and D_i were adjusted to give a solitary wave conduction velocity of 0.5 mm/ms [8]. Further, the pseudo-ECG was simulated using the extracellular potentials and assuming the recording electrode to be grounded [12]. The 1D virtual strands thus constructed was seen to be capable of reproducing the QRS and T complexes representing the ventricular

component of clinical ECG. In the 1D strand simulations, one end of the tissue was paced to induce excitations propagating through the strand. Stable excitations were elicited by pacing the strand using 20 such stimuli at a pacing rate of 1 Hz. The CV, APD_{90} profile, and ECG profile produced by the 20th wave propagation were recorded for further analysis. Multiple simulations using the 1D strand were conducted in a large range of $[K^+]_o$ values. Finally, the CV, APD_{90}, and ECG features were correlated to $[K^+]_o$. Finally, the effects of heterogeneous gap junctional coupling were simulated as a non-uniform distribution of D_e and D_i in Eq. (1) under various $[K^+]_o$ values. A step change reduction of the diffusion was implemented.

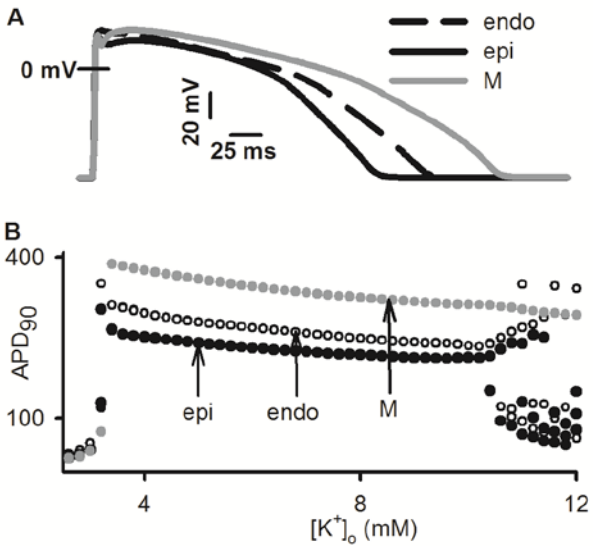

Figure 1. Basal AP profiles, and APD_{90} dependence on $[K^+]_o$. A: AP profiles of endo, M, and epi cell types in the ORD [6] model at $[K^+]_o$ = 5.4 mM. B: APD_{90} of the cell types as a function of $[K^+]_o$.

The cell model ODEs were solved using a higher order implicit Backward Difference Formula method that uses Newton iterations. The reaction current from the cell model solution was then used in the PDE in equation (1), which was solved using a Crank-Nicolson 3-point stencil finite difference discretization. The resulting systems were solved in a single direct step using Gaussian elimination. Such an implicit solution imparts unconditional stability as well as improved accuracy to the numerical solution [7, 11]. The Crank-Nicolson discretization has the further advantage of being second order accurate in time. Such direct solution is practical only for the 1D model under consideration. The time step in all simulations was taken to be 0.05 ms, while the space step was taken to be 0.1 mm in Eq. (1). The cell as well as 1D models in themselves do not present computational challenges. The numerous simulations for the parameter sweeps were carried out using a distributed HPC cluster resource in Liverpool.

3. Results

APs after 1000 s stimulation at 1 Hz pacing were used to characterize stable AP characteristics (Figure 1). The basal APD_{90} at $[K^+]_o$ = 5.4 mM was found to be 230 ms (epi), 272 ms (endo), and 332 ms (M) respectively (Figure 1A). At lower values of $[K^+]_o$ (Figure 1B) representing the hypokalemic condition, APD_{90} was seen to increase. AP failed to repolarize for $[K^+]_o$ under 3.2 mM. At higher values $[K^+]_o$ values representing hyperkalemic conditions, APD_{90} reduced. The cell models produced aperiodic APs for $[K^+]_o$ values over 10.4 mM. At high pacing rates, dynamic restitution shows alternans in the cell models (Figure 2). Under basal conditions ($[K^+]_o$ = 5.4 mM), the onset of alternans or aperiodic AP excitations was at PCL less than or equal to 270 ms. Under hypokalemic conditions ($[K^+]_o$ = 3.8 mM), the onset of alternans was at PCL = 310 ms. Under hyperkalemic conditions ($[K^+]_o$ = 9 mM), alternans onset PCL was found to be 290 ms.

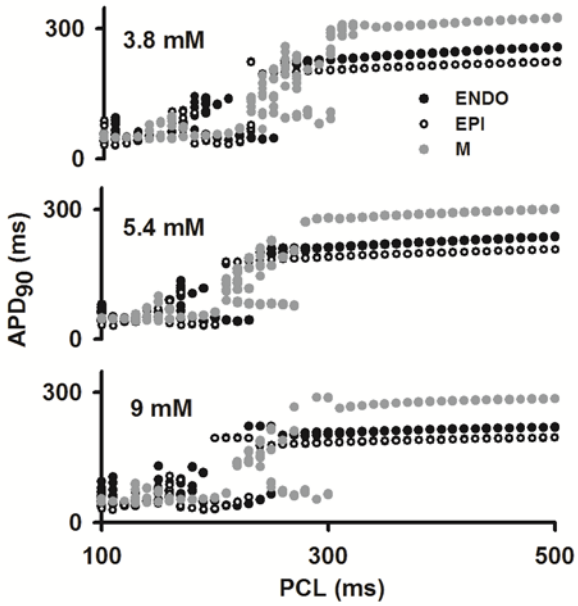

Figure 2. Dynamic restitution under hyperkalemic (top panel), basal (middle panel) and hyperkalemic conditions (bottom panel) showing alternans and aperiodic excitations at high pacing rates.

In the 1D strand model with uniform gap junctional coupling, the correlation between $[K^+]_o$ and CV was quantified (Figure 3). In both cases of hypokalemia and hyperkalemia, CV in the strand was reduced as compared to the basal CV of 0.5 mm/ms for $[K^+]_o$ = 5.4 mM. In contrast to clinical observations, excitation propagation could not be elicited for $[K^+]_o$ more than 6 mM.

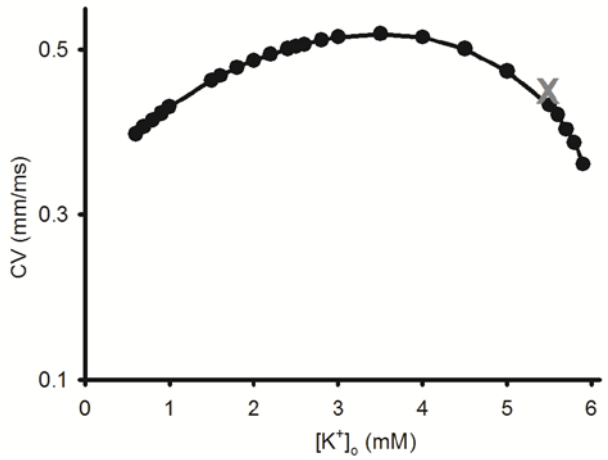

Figure 3. Conduction velocity as a function of serum potassium concentration. The gray "X" denotes CV at the physiological $[K^+]_o$ value of 5.4 mM.

To analyse the correlation between $[K^+]_o$ and ECG, the 1D strand with uniform gap junctional coupling was used in a parameter sweep simulation. T waves in the simulated ECG were then analysed for T wave amplitude and T wave repolarization slope (Figure 4).

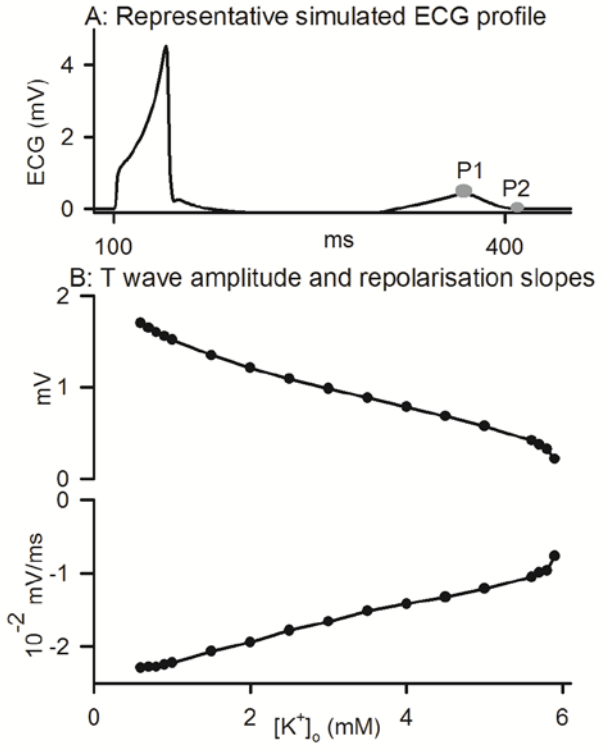

Figure 4. Correlation of ECG with $[K^+]_o$. A: Representative ECG profile indicating the peak of ECG T wave (P1) and points in the ECG used to compute descending T wave slope using: (P2 – P1)/(tP2 – tP1).

In vitro experimental observations have shown the existence of "islands" of mid cell types in human ventricular wall [8]. To incorporate the augmented APD_{90} dispersion due to such electrophysiological heterogeneity was implemented in the 1D strand. It was done by incorporating heterogeneous gap junctional coupling, i.e. spatially dependent D_e and D_i in Eq. (1). A step change reduction of the diffusion was implemented. As shown in Figure 5, the APD_{90} dispersion (defined as the difference between longest and shortest APD_{90} in the strand) was unaffected. The effects of reducing the $[K^+]_o$ was the increase the dispersion by 7%. Upon increasing $[K^+]_o$, the dispersion was 18%.

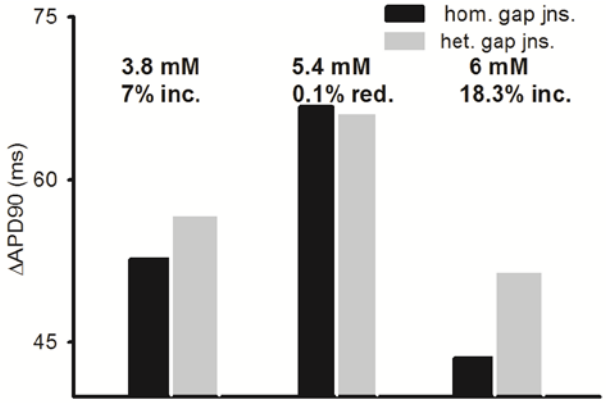

Figure 5. Increase of APD_{90} dispersion due to altered $[K^+]_o$ and step change heterogeneous gap junctional coupling.

4. Conclusions and discussion

The simulations provide insights into the proarrhythmic effects of $[K^+]_o$ on cell and tissue electrical behaviour. A reduced $[K^+]_o$ increases APD_{90} indicating a propensity towards spontaneous after depolarization. An increased $[K^+]_o$ reduces APD_{90} indicating a propensity towards sustaining mother rotors leading to persistent fibrillation. Although not confirmed in the 1D model, the cell models indicate the increased incidence of alternans and aperiodic AP excitations due to altered $[K^+]_o$ which may lead to functional heterogeneity based fibrillation in the human ventricles [13]. A reduced CV is known to favour sustained re-entry and fibrillation, which is caused by altered $[K^+]_o$. The biphasic reduction of CV due to $[K^+]_o$ is consistent with previous reports [14, 15]. Importantly, the 1D strand has demonstrated a conclusive correlation between ECG features of T wave amplitude and T wave repolarization slope with $[K^+]_o$. This may be used clinically in non-invasive diagnosis procedures. Finally, incorporating a realistic heterogeneous inter-cellular coupling was seen to lead to an increased APD_{90} dispersion. Such increased electrophysiological

heterogeneity is known to lead to increased propensity of fibrillation.

The model limitations are as follows. Although the ORD model is extensively validated and biophysically detailed, its capability of reproducing AP profiles in the complete range of clinically observed $[K^+]_o$ (between 2 mM to 13 mM) remains limited. The incorporation of the ORD model into the 1D strand further limits its capability to sustain conduction propagation in the physiological range of $[K^+]_o$. The electrical heterogeneity incorporated into the 1D model is based on limited experimental data, which may affect model behaviour and its ability to reproduce the effects of $[K^+]_o$ on ECG. The method of solving the PDE by Gaussian elimination is restricted to 1D problems and may not be extensible to higher spatial dimensions as the systems matrix in 2 and 3 dimensional problems is prohibitively large. Nonetheless, the direct solver method used in this study eliminates any operator splitting errors.

A natural extension of this work would be to study the effects of realistic fiber orientation and anatomical geometry in combination with the $[K^+]_o$ alterations [5]. The roles of gap junctional heterogeneity needs to be further investigated as the present model does not reproduce the experimentally observed large APD dispersion in human ventricles [8].

Acknowledgements

This work was supported by the Italy CHIRON project, HPC Europa 2011 visiting fellowship grant, EPSRC grant (EP/I029664/1), and PRACE Introductory HPC Access (PRPB09, 2012).

References

[1] Green D, Roberts P R, New D I and Kalra P A Sudden cardiac death in hemodialysis patients: an in-depth review. American journal of kidney diseases : the official journal of the National Kidney Foundation. 2011; 57: 921-9

[2] Santoro A, Mancini E, Gaggi R, Cavalcanti S, Severi S, Cagnoli L, Badiali F, Perrone B, London G, Fessy H, Mercadal L and Grandi F Electrophysiological response to dialysis: the role of dialysate potassium content and profiling. Contrib Nephrol. 2005; 149: 295-305

[3] Severi S, Corsi C and Cerbai E From in vivo plasma composition to in vitro cardiac electrophysiology and in silico virtual heart: the extracellular calcium enigma. Philos Transact A Math Phys Eng Sci. 2009; 367: 2203-23

[4] Severi S, Pogliani D, Fantini G, Fabbrini P, Vigano M R, Galbiati E, Bonforte G, Vincenti A, Stella A and Genovesi S Alterations of atrial electrophysiology induced by electrolyte variations: combined computational and P-wave analysis. Europace. 2010; 12: 842-9

[5] Krueger M W, Severi S, Rhode K, Genovesi S, Weber F M, Vincenti A, Fabbrini P, Seemann G, Razavi R and Dossel O Alterations of atrial electrophysiology related to hemodialysis session: insights from a multiscale computer model. J Electrocardiol. 2011; 44: 176-83

[6] O'Hara T, Virag L, Varro A and Rudy Y Simulation of the undiseased human cardiac ventricular action potential: model formulation and experimental validation. PLoS Comput Biol. 2011; 7 e1002061

[7] Keener J P and Bogar K A numerical method for the solution of the bidomain equations in cardiac tissue. Chaos. 1998; 8: 234-41

[8] Glukhov A V, Fedorov V V, Lou Q, Ravikumar V K, Kalish P W, Schuessler R B, Moazami N and Efimov I R Transmural dispersion of repolarization in failing and nonfailing human ventricle. Circ Res. 2010; 106: 981-91

[9] Seemann G, Sachse F B, Karl M, Weiss D L, Heuveline V and Dossel O Framework for Modular, Flexible and Efficient Solving the Cardiac Bidomain Equations Using PETSc. Math Indust. 2010; 15: 363-9

[10] Vigmond E J, Weber dos Santos R, Prassl A J, Deo M and Plank G Solvers for the cardiac bidomain equations. Prog Biophys Mol Biol. 2008; 96: 3-18

[11] Zhang Y, Xia L and Hou G H 2006 *Computational Intelligence and Bioinformatics, Pt 3, Proceedings,* (Berlin: Springer-Verlag Berlin) pp 571-81

[12] Plonsey R and Barr R C Mathematical modeling of electrical activity of the heart. J Electrocardiol. 1987; 20: 219-26

[13] Myles R C, Burton F L, Cobbe S M and Smith G L Alternans of action potential duration and amplitude in rabbits with left ventricular dysfunction following myocardial infarction. J Mol Cell Cardiol. 2011; 50: 510-21

[14] Buchanan J W, Jr., Saito T and Gettes L S The effects of antiarrhythmic drugs, stimulation frequency, and potassium-induced resting membrane potential changes on conduction velocity and dV/dtmax in guinea pig myocardium. Circ Res. 1985; 56: 696-703

[15] Shaw R M and Rudy Y Electrophysiologic effects of acute myocardial ischemia. A mechanistic investigation of action potential conduction and conduction failure. Circ Res. 1997; 80: 124-38

Address for correspondence.
Name: Sanjay Kharche
Address: University of Liverpool, Liverpool, L69 7ZL,UK
E-mail address: Sanjay.Kharche@liverpool.ac.uk